

Infrared transmission study of crystal-field excitations in Al- and Sr-doped $\text{Pr}_{1+x}\text{Ba}_{2-x}\text{Cu}_3\text{O}_6$

D. Barba* and S. Jandl

Centre de Recherche sur les Propriétés Electroniques des Matériaux Avancés, Département de Physique, Université de Sherbrooke, Sherbrooke, Canada J1K 2R1

V. Nekvasil, M. Maryško, and K. Jurek

Institute of Physics, Czech Academy of Sciences, Cukrovarnická 10, 162 53 Praha 6, Czech Republic

M. Diviš

Department of Electron Systems, Charles University, Ke Karlovu 2, 121 16 Praha 2, Czech Republic

Th. Wolf

Forschungszentrum Karlsruhe, Institut für Festkörperphysik, D-76021 Karlsruhe, Germany

(Received 12 September 2003; published 30 January 2004)

Absorption bands corresponding to the crystal-field excitations in $\text{Pr}_{1.05}\text{Ba}_{1.88}\text{Cu}_{2.39}\text{Al}_{0.34}\text{O}_{6+y}$ and $\text{Pr}_{0.93}\text{Ba}_{1.93}\text{Sr}_{0.13}\text{Mg}_{0.05}\text{Cu}_{2.74}\text{O}_{6+y}$ (where $y \sim 0$) have been observed by Raman scattering and infrared transmission spectroscopy. These excitations are assigned to transitions occurring from the two lowest-energy levels of the 3H_4 multiplet to the excited multiplets 3H_5 , 3H_6 , 3F_2 , and 3F_3 of Pr^{3+} ions located in their D_{4h} -symmetry sites. The spectra exhibit additional bands consistent with the presence of Pr^{3+} ions in the C_{4v} -symmetry Ba sites, as well as various defects associated with disorder. This analysis confirms that the phenomenological crystal-field parameters follow the trends reported in $\text{NdBa}_2\text{Cu}_3\text{O}_6$ and $\text{SmBa}_2\text{Cu}_3\text{O}_6$. A spectral splitting of the Γ_5 levels is observed at low temperature and indicates Pr-Cu exchange interaction. Al doping results in the expected inversion of the Γ_5 - Γ_1 symmetry sequence of the quasitriplet ground state, in accordance with the magnetic-susceptibility anisotropy measurements.

DOI: 10.1103/PhysRevB.69.024528

PACS number(s): 74.72.Jt, 78.30.Hv, 75.10.Dg, 71.70.Ej

I. INTRODUCTION

The magnetic and electronic properties of $\text{Pr}_{1+x}\text{Ba}_{2-x}\text{Cu}_3\text{O}_{6+y}$ clearly differ from those of the other $\text{RE}_{1+x}\text{Ba}_{2-x}\text{Cu}_3\text{O}_{6+y}$ (RE—rare earth) compounds. Namely, the antiferromagnetic (AFM) ordering of the RE^{3+} sublattice occurs at T_N ranging between 12 ($y = 0$) and 17 K ($y = 1$) in $\text{Pr}_{1+x}\text{Ba}_{2-x}\text{Cu}_3\text{O}_{6+y}$, whereas this Néel temperature is an order of magnitude lower in $\text{NdBa}_2\text{Cu}_3\text{O}_6$ and $\text{SmBa}_2\text{Cu}_3\text{O}_6$.^{1,2} Moreover, the $\text{PrBa}_2\text{Cu}_3\text{O}_7$ samples do not superconduct and the increase of the Pr concentration leads to a drastic reduction of the critical temperature in the superconducting $\text{RE}_{1-x}\text{Pr}_x\text{Ba}_2\text{Cu}_3\text{O}_7$ systems.³ Nevertheless, it has been argued that $\text{PrBa}_2\text{Cu}_3\text{O}_7$ superconducts at a critical temperature of roughly 90 K, if the sample is almost free of Pr in Ba site defects.^{4,5} These defects are difficult to detect by neutron or x-ray-diffraction measurements since Pr and Ba have the same neutron-scattering length and close atomic numbers. It has been established that the particular properties of Pr-based materials are either caused by the enhanced oxygen-mediated interaction between the Pr^{3+} ions and their neighboring $\text{Cu}(2)^{2+}$ ions,^{6,7} or by the crystal disorder associated with the chemical Pr/Ba substitution.^{4,5} Recently, the resistivity and the thermopower measurements performed in $\text{Y}_{1-x}\text{Pr}_x\text{Ba}_2\text{Cu}_3\text{O}_7$ and $\text{SmBa}_{2-x}\text{Pr}_x\text{Cu}_3\text{O}_7$ compounds revealed that their electrical conductivity is less affected by possible Pr-4*f*/O-2*p* orbital hybridization than by the presence of Pr in Ba sites,⁸ which is responsible for a decrease of

the charge-carrier density.⁹ On the other hand, the inelastic neutron-scattering (INS) measurements show that the Nd/Ba substitution gives rise to an effective ferromagnetic coupling between the Cu^{2+} ions of the $\text{Cu}(2)\text{O}(2,3)$ planes and the $\text{Cu}(1)\text{-O}(1)$ chains in $\text{Nd}_{1+x}\text{Ba}_{2-x}\text{Cu}_3\text{O}_{6+y}$.¹⁰ Such magnetic reordering leads to a significant drop of T_N in the nonstoichiometric compounds and is adverse to the formation of the superconducting state in the highly oxygenated materials.

Recently, infrared transmission spectroscopy has been successfully used in the characterization of the crystal-field (CF) interaction at the regular RE sites located between the two adjacent conducting planes in $\text{NdBa}_2\text{Cu}_3\text{O}_6$ and $\text{Sm}_{1+x}\text{Ba}_{2-x}\text{Cu}_3\text{O}_6$ ($x = 0.01, 0.03, 0.05, \text{ and } 0.11$).^{11,12} In spite of the infrared inactive D_{4h} -symmetry site of the rare earth ions, the *f-f* transitions become infrared active due to the loss of the inversion center resulting from in-chain oxygen excess and RE/Ba substitution. In addition to complementing the results obtained by the INS techniques,^{13,14} the infrared transmission measurements in $\text{NdBa}_2\text{Cu}_3\text{O}_6$ and $\text{Sm}_{1+x}\text{Ba}_{2-x}\text{Cu}_3\text{O}_6$ have provided a precise description of the CF excitations in the 1000–10 000 cm^{-1} range and a clear indication of Nd/Ba and Sm/Ba substitutions. These investigations, including the superposition model and the density-functional theory based calculations, allow a detailed understanding of thermodynamical properties such as magnetic susceptibility and specific heat. The INS studies of $\text{PrBa}_2\text{Cu}_3\text{O}_{6+y}$ available in the literature led however to con-

flicting analysis.^{15–18} Although all groups agree with the theoretically “quasitriplet” ground state of Pr^{3+} , separated by the energy gap of several hundreds of cm^{-1} from the 3H_4 multiplet,¹⁹ the detailed CF splitting strongly depends on the sample composition and the growing process.

This paper deals with the IR transmission study of insulating $\text{Pr}_{1.05}\text{Ba}_{1.88}\text{Cu}_{2.39}\text{Al}_{0.34}\text{O}_{6+y}$ and $\text{Pr}_{0.93}\text{Ba}_{1.93}\text{Sr}_{0.13}\text{Mg}_{0.05}\text{Cu}_{2.74}\text{O}_{6+y}$ compounds, where $y \sim 0$, in the 2000–7000 cm^{-1} range. For each sample, we report a systematic study of intermultiplet f - f transitions from the two lowest levels of the 3H_4 ground-state multiplet to the 3H_5 , 3H_6 , 3F_2 , and 3F_3 excited multiplets, in order to determine a reliable set of CF parameters. Also, our work focuses on the effects of the Pr/Ba substitution and the Al doping, and allows to reproduce the magnetic-susceptibility anisotropy.

II. EXPERIMENTS

$\text{Pr}_{1.05}\text{Ba}_{1.88}\text{Cu}_{2.39}\text{Al}_{0.34}\text{O}_{6+y}$ and $\text{Pr}_{0.93}\text{Ba}_{1.93}\text{Sr}_{0.13}\text{Mg}_{0.05}\text{Cu}_{2.74}\text{O}_{6+y}$ single crystals were grown in two different laboratories by the self-flux method,^{20,21} using Al_2O_3 and MgO crucibles, respectively. Both samples, with initial oxygen contents equal to 6.35 (sample 1) and 6.24 (sample 2), were annealed in flowing argon at $T = 700^\circ\text{C}$ for 96 h, thus ensuring optimal oxygen reduction. Their tetragonal symmetry as well as their orientation were checked by Raman spectroscopy. The following lattice parameters : $a = 3.93 \text{ \AA}$, $c = 11.78 \text{ \AA}$ for $\text{Pr}_{1.05}\text{Ba}_{1.88}\text{Cu}_{2.39}\text{Al}_{0.34}\text{O}_{6+y}$ and $a = 3.91 \text{ \AA}$, $c = 11.72 \text{ \AA}$ for $\text{Pr}_{0.93}\text{Ba}_{1.93}\text{Sr}_{0.13}\text{Mg}_{0.05}\text{Cu}_{2.74}\text{O}_{6+y}$ were obtained by x-ray diffraction measurements at room temperature. Their nominal composition was determined by electron microprobe x-ray analysis using wavelength dispersive spectrometers (WDS—JXA 733 of JEOL). Samples were analyzed as grown prior to reduction, on natural shiny surfaces and also on optically polished surfaces to confirm previous results. Atomic concentrations were calculated supposing twelve atoms per unit cell.

Low-temperature Raman back-scattering studies were performed using a LABRAM-800 confocal system equipped with a nitrogen-cooled charge-coupled-device (CCD) detector and a 5 mW 633 nm He-He laser line polarized perpendicular to the c axis, focused to a few microns spot diameter on the sample.

The infrared measurements were carried out with a fast-Fourier-transform interferometer (BOMEM DA3.002), using a quartz halogen lamp, an InSb detector, and a CaF_2 beam splitter. $1 \times 0.5 \times 0.1 \text{ mm}^3$ $\text{Pr}_{1.05}\text{Ba}_{1.88}\text{Cu}_{2.39}\text{Al}_{0.34}\text{O}_{6+y}$ and $\text{Pr}_{0.93}\text{Ba}_{1.93}\text{Sr}_{0.13}\text{Mg}_{0.05}\text{Cu}_{2.74}\text{O}_{6+y}$ single crystals were mounted on the cold finger of a helium-cooled flow-through cryostat and 1 cm^{-1} resolution transmittance spectra were recorded with the ac plane perpendicular to the direction of the unpolarized incident beam.

The magnetic susceptibility of crystalline platelets were measured by using a superconducting quantum interference device magnetometer quantum design MPM-5S in the temperature range from 4.5 K to 300 K, with a 0.1 T static

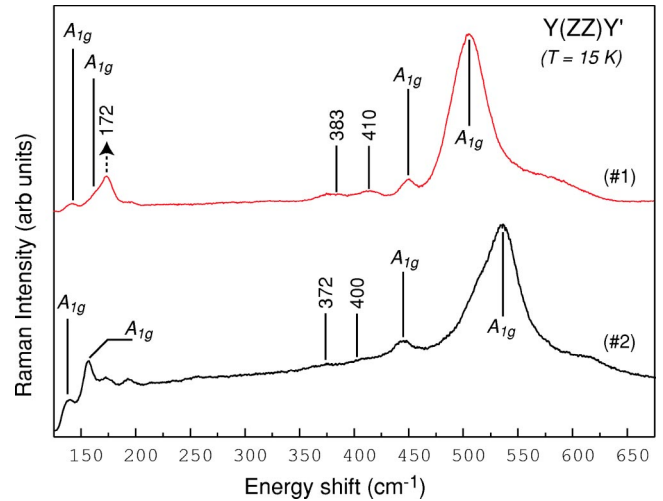


FIG. 1. Raman spectra of $\text{Pr}_{1.05}\text{Ba}_{1.88}\text{Cu}_{2.39}\text{Al}_{0.34}\text{O}_{6+y}$ (sample 1) and $\text{Pr}_{0.93}\text{Ba}_{1.93}\text{Sr}_{0.13}\text{Mg}_{0.05}\text{Cu}_{2.74}\text{O}_{6+y}$ (sample 2), at $T = 15 \text{ K}$, in the $y(zz)\bar{y}$ configuration.

magnetic field oriented either parallel or perpendicular to the CuO_2 planes.

III. RESULTS

The Raman measurements of the $\text{Pr}_{1.05}\text{Ba}_{1.88}\text{Cu}_{2.39}\text{Al}_{0.34}\text{O}_{6+y}$ (sample 1) and the $\text{Pr}_{0.93}\text{Ba}_{1.93}\text{Sr}_{0.13}\text{Mg}_{0.05}\text{Cu}_{2.74}\text{O}_{6+y}$ (sample 2) crystals in the 125–625 cm^{-1} range are presented in Fig. 1. These spectra are obtained in the $y(zz)\bar{y}$ configuration at $T = 15 \text{ K}$. We identify four A_{1g} phonons around 130, 170, 450, and 500 cm^{-1} consistent with previous reports.^{22,23} The additional peak observed at 172 cm^{-1} in $\text{Pr}_{1.05}\text{Ba}_{1.88}\text{Cu}_{2.39}\text{Al}_{0.34}\text{O}_{6+y}$ is due to the Al/Cu(1) substitution.²⁴ We associate the 383 and 410 cm^{-1} lines in sample 1 and the 372 and 400 cm^{-1} lines in sample 2 to the f - f transitions occurring from the ground state to the 3rd and 4th excited level of the 3H_4 multiplet, respectively.

Figure 2 shows the infrared transmission spectra obtained at $T = 10$ and 78 K in the 2225–2825 cm^{-1} range, where the $^3H_4 \rightarrow ^3H_5$ transitions occur. In sample 1, five f - f transitions are observed at 2260, 2285, 2346/59, 2580, and 2665 cm^{-1} at $T = 10 \text{ K}$, with a satellite absorption band at $T = 78 \text{ K}$ associated with the double feature at 2346/59 cm^{-1} . In sample 2, six CF excitations at 2250, 2273, 2242/56, 2557, 2667, and 2806 cm^{-1} are observed. We note the presence of two additional absorption bands at $T = 78 \text{ K}$, whose energies are located 10 cm^{-1} above the 2242/56 and 2557 cm^{-1} levels. Around 2290 and 2450 cm^{-1} , the vertical arrows point out two weak absorption bands in $\text{Pr}_{0.93}\text{Ba}_{1.93}\text{Sr}_{0.13}\text{Mg}_{0.05}\text{Cu}_{2.74}\text{O}_{6+y}$, while the filled circles designate regions where defects have been observed in $\text{NdBa}_2\text{Cu}_3\text{O}_6$ and $\text{Sm}_{1+x}\text{Ba}_{2-x}\text{Cu}_3\text{O}_6$.^{11,12} Between 4100 and 5300 cm^{-1} , in Figs. 3(a) and 3(b), the $^3H_4 \rightarrow ^3H_6$ transitions are presented. CF excitations are associated with the absorption bands observed at 4293, 4332, 4504, 4615, 4811, 4989, 5067, and 5105 cm^{-1} in sample 1, and at 4287, 4336, 4499, 4611, 4808, 5012, 5060, and 5114 cm^{-1} in sample 2.

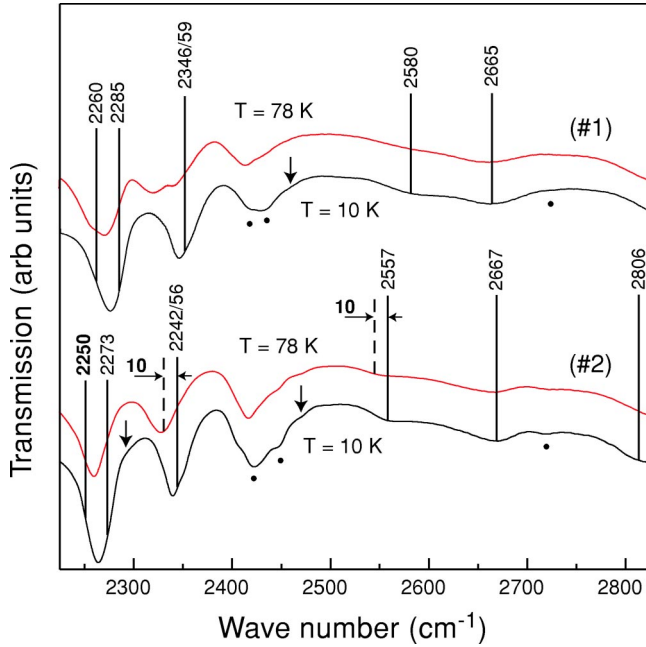


FIG. 2. IR transmission spectra at $T=10$ and 78 K, across ac -oriented platelets of $\text{Pr}_{1.05}\text{Ba}_{1.88}\text{Cu}_{2.39}\text{Al}_{0.34}\text{O}_{6+y}$ (sample 1) and $\text{Pr}_{0.93}\text{Ba}_{1.93}\text{Sr}_{0.13}\text{Mg}_{0.05}\text{Cu}_{2.74}\text{O}_{6+y}$ (sample 2) in the $2225\text{--}2825\text{ cm}^{-1}$ range. Vertical lines and vertical arrows indicate Pr^{3+} CF excitations associated with D_{4h} - and C_{4v} -symmetry sites, respectively. (●) designates absorption bands also observed in $\text{NdBa}_2\text{Cu}_3\text{O}_6$ (Ref. 11) and $\text{Sm}_{1+x}\text{Ba}_{2-x}\text{Cu}_3\text{O}_6$ (Ref. 12).

At $T=78$ K, the spectra exhibit additional bands with energies shifted $\sim 7\text{ cm}^{-1}$ and $\sim 10\text{ cm}^{-1}$ from bands measured at $T=10$ K. A far infrared study of polycrystalline $\text{PrBa}_2\text{Cu}_3\text{O}_6$ performed by Mukhin *et al.*²⁵ has indicated the presence of a weak and broad absorption band around 15 cm^{-1} at $T < 70$ K, attributed to electronic transitions between the low-energy CF levels of Pr^{3+} . The vertical arrows locate bands with larger intensity in $\text{Pr}_{0.93}\text{Ba}_{1.93}\text{Sr}_{0.13}\text{Mg}_{0.05}\text{Cu}_{2.74}\text{O}_{6+y}$ and (*) designates defects. ${}^3H_4 \rightarrow {}^3F_2$ transitions, which cover the $5250\text{--}5850\text{ cm}^{-1}$ range are shown in Fig. 4. These excitations are, respectively, ascribed to the bands observed at 5471 , $5516/24$, 5601 , and 5614 cm^{-1} in sample 1, and at 5471 , $5517/28$, 5598 , and 5625 cm^{-1} in sample 2. Finally, we assign the lines at 6527 , 6630 cm^{-1} in $\text{Pr}_{1.05}\text{Ba}_{1.88}\text{Cu}_{2.39}\text{Al}_{0.34}\text{O}_{6+y}$ and 6530 , 6640 cm^{-1} in $\text{Pr}_{0.93}\text{Ba}_{1.93}\text{Sr}_{0.13}\text{Mg}_{0.05}\text{Cu}_{2.74}\text{O}_{6+y}$ (Fig. 5) to the ${}^3H_4 \rightarrow {}^3F_3$ transitions.

IV. DISCUSSION

We analyze our transmission measurements in terms of the CF interaction, which is the strongest perturbation of free-ion $4f$ electron states of the RE^{3+} in the cuprates. The CF Hamiltonian can be written as

$$H_{CF} = \sum_{k,q} B_{kq} [C_q^{(k)} + C_q^{(k)}], \quad (1)$$

where the $C_q^{(k)}$ and B_{kq} Wybourne operators correspond to the q th component of the spherical tensor operator of rank k

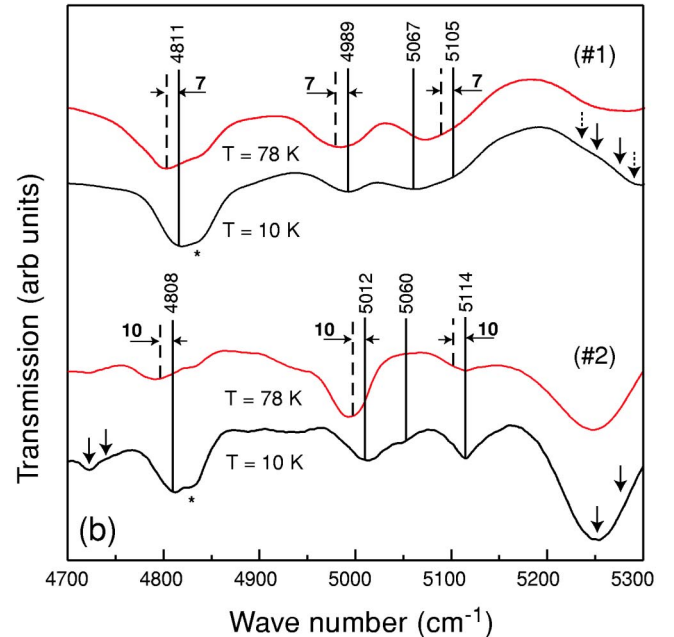
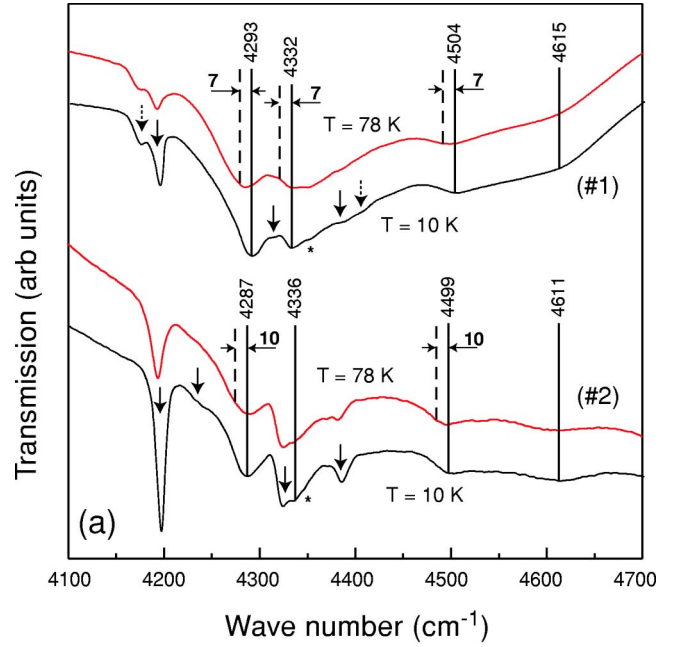


FIG. 3. ${}^3H_4 \rightarrow {}^3H_6$ CF transitions in $\text{Pr}_{1.05}\text{Ba}_{1.88}\text{Cu}_{2.39}\text{Al}_{0.34}\text{O}_{6+y}$ (sample 1) and $\text{Pr}_{0.93}\text{Ba}_{1.93}\text{Sr}_{0.13}\text{Mg}_{0.05}\text{Cu}_{2.74}\text{O}_{6+y}$ (sample 2), in the $4100\text{--}4700\text{ cm}^{-1}$ (a) and $4700\text{--}5300\text{ cm}^{-1}$ ranges. Vertical lines and vertical arrows indicate Pr^{3+} CF excitations associated with D_{4h} - and C_{4v} -symmetry sites, respectively. The dashed arrows are associated with Al doping in sample 1, and (*) corresponds to local defects.

and the so-called CF parameters, respectively.²⁶ In the D_{4h} -symmetry regular site of Pr^{3+} , as well as in the C_{4v} -symmetry Pr/Ba substitution site in nonstoichiometric $\text{Pr}_{1+x}\text{Ba}_{2-x}\text{Cu}_3\text{O}_{6+y}$, only five CF parameters B_{20} , B_{40} , B_{44} , B_{60} , and B_{64} are nonzero.²⁷ Following the standard procedure (for a recent survey of the CF data reported for the RE cuprates, see Refs. 27 and 28), their values are determined by solving numerically the *inverse secular problem*

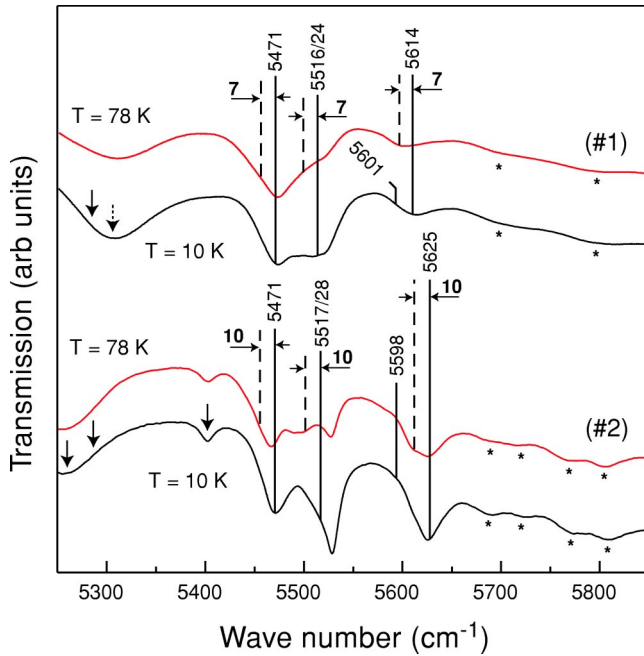


FIG. 4. IR absorption bands due to ${}^3H_4 \rightarrow {}^3F_2$ CF transitions from Pr^{3+} ions in the regular site (lines) and the Pr/Ba site (arrows) in $\text{Pr}_{1.05}\text{Ba}_{1.88}\text{Cu}_{2.39}\text{Al}_{0.34}\text{O}_{6+y}$ (sample 1) and $\text{Pr}_{0.93}\text{Ba}_{1.93}\text{Sr}_{0.13}\text{Mg}_{0.05}\text{Cu}_{2.74}\text{O}_{6+y}$ (sample 2), in the $5250\text{--}5850\text{ cm}^{-1}$ range. (*) designates defects.

where the CF levels deduced from the experimental data are taken to be the eigenvalues of the CF Hamiltonian.²⁹

Regarding the D_{4h} -symmetry site, our CF analysis has been performed in two steps. First, we have restricted the

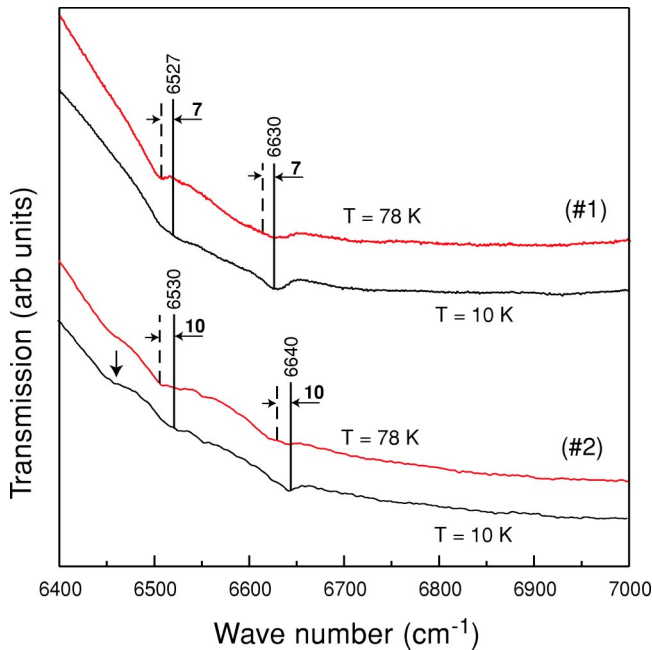


FIG. 5. IR absorption bands due to ${}^3H_4 \rightarrow {}^3F_3$ CF transitions from Pr^{3+} ions in the regular site (lines) and the Pr/Ba site (arrows) in $\text{Pr}_{1.05}\text{Ba}_{1.88}\text{Cu}_{2.39}\text{Al}_{0.34}\text{O}_{6+y}$ (sample 1) and $\text{Pr}_{0.93}\text{Ba}_{1.93}\text{Sr}_{0.13}\text{Mg}_{0.05}\text{Cu}_{2.74}\text{O}_{6+y}$ (sample 2) in the $6400\text{--}7000\text{ cm}^{-1}$ range.

fitting procedure to the 13 (sample 1) and 14 (sample 2) bands that present a satellite absorption at $T=78\text{ K}$, using the CF parameters obtained for the regular site of Nd^{3+} in $\text{NdBa}_2\text{Cu}_3\text{O}_6$ as an initial estimate.¹¹ We conjecture that these satellite lines correspond to transitions occurring from the first excited level of the 3H_4 multiplet located at $\sim 10\text{ cm}^{-1}$ above the ground state. We have then successively included the energies of the bands close to the levels predicted by the previous fit in the calculation. This procedure was iterated for each multiplet till the criterion of convergence was satisfied. The final best-fit parameters for the regular D_{4h} -symmetry sites are given in Table I for each sample. Their corresponding CF levels are reported in Table II for the multiplets 3H_4 , 3H_5 , 3H_6 , 3F_2 , and 3F_3 . The standard deviations between the calculated energies and the CF levels observed by Raman and IR transmittance measurements are 4.06 and 4.33 cm^{-1} for $\text{Pr}_{1.05}\text{Ba}_{1.88}\text{Cu}_{2.39}\text{Al}_{0.34}\text{O}_{6+y}$ and $\text{Pr}_{0.93}\text{Ba}_{1.93}\text{Sr}_{0.13}\text{Mg}_{0.05}\text{Cu}_{2.74}\text{O}_{6+y}$, respectively. The free-ion levels, which vary with the CF parameters in the fitting procedure, are 0 , 2123 , 4340 , 4793 , and 6141 cm^{-1} for $\text{Pr}_{1.05}\text{Ba}_{1.88}\text{Cu}_{2.39}\text{Al}_{0.34}\text{O}_{6+y}$ (sample 1) and 0 , 2119 , 4337 , 4808 , and 6148 cm^{-1} for $\text{Pr}_{0.93}\text{Ba}_{1.93}\text{Sr}_{0.13}\text{Mg}_{0.05}\text{Cu}_{2.74}\text{O}_{6+y}$ (sample 2). These values are close to the free-ion levels of Pr^{3+} in Pr_2CuO_4 .³⁰

Since the Pr/Ba substitution depends on the crystal growing process, the spectral weight of the bands relative to the presence of Pr^{3+} in the Ba sites can drastically vary with the sample origin. According to Muroi and co-workers^{31,32}, a small amount of Sr seems to favor the Pr/Ba substitution, thus leading to stronger spectral absorption bands in $\text{Pr}_{0.93}\text{Ba}_{1.93}\text{Sr}_{0.13}\text{Mg}_{0.05}\text{Cu}_{2.74}\text{O}_{6+y}$. This feature allows us to ascribe the lines pointed by a vertical arrow in Figs. 2–5 to the irregular C_{4v} -symmetry site of Pr. In the two last columns of Table II, the energy of these transitions are compared to the calculation performed for the C_{4v} -symmetry site, using the previously determined free-energy levels and the CF parameters reported in the 6th column of Table I. Presuming that the variation of B_{kq} across the RE series is smooth, we have derived this set from a former study of $\text{SmBa}_2\text{Cu}_3\text{O}_6$, reported in the 7th column of Table I.¹²

Our CF analysis of Pr^{3+} is based on 22 and 23 observed f - f transitions that involve the five lowest multiplets ${}^3H_{4-6}$ and ${}^3F_{2-3}$. The INS studies of $\text{PrBa}_2\text{Cu}_3\text{O}_{6+y}$ provide more limited data since they have been restricted to the transitions within the 3H_4 ground-state multiplet.^{15,18,33} The experimental CF levels obtained for $y \sim 1$ have been determined at 0 , 32 , 363 , 403 , 524 , 645 , 686 , and 847 cm^{-1} and at 0 , 12 , 27 , 508 , 547 , 669 , and 786 cm^{-1} by Soderholm *et al.*¹⁵ and Hilscher *et al.*,¹⁸ respectively. The ground-state CF splitting magnitudes reported by Boothroyd *et al.*³³ and Hilscher *et al.*¹⁸ are very close. The only data available for $y \sim 0$ have been published by Hilscher *et al.*¹⁸, locating the CF levels of the 3H_4 multiplet at 0 , 14 , 27 , 492 , 522 , 608 , and 678 cm^{-1} . The differences between various CF analysis performed by INS is due to discrepancies in the broadband assignments. For example, bands around 400 cm^{-1} have been assigned to CF excitations by Soderholm *et al.*,¹⁵ whereas a similar

TABLE I. Pr^{3+} ion CF parameters (in cm^{-1}) for $\text{Pr}_{1.05}\text{Ba}_{1.88}\text{Cu}_{2.39}\text{Al}_{0.34}\text{O}_{6+y}$ (sample 1), $\text{Pr}_{0.93}\text{Ba}_{1.93}\text{Sr}_{0.13}\text{Mg}_{0.05}\text{Cu}_{2.74}\text{O}_{6+y}$ (sample 2), $\text{NdBa}_2\text{Cu}_3\text{O}_6$ (Ref. 11), and $\text{SmBa}_2\text{Cu}_3\text{O}_6$ (Ref. 12). Given in brackets are the mean errors associated with the fitting parameters.

B_{kq}	D_{4h} -symmetry site				C_{4v} -symmetry	
	Sample 1 (fit)	Sample 2 (fit)	$\text{NdBa}_2\text{Cu}_3\text{O}_6$	$\text{SmBa}_2\text{Cu}_3\text{O}_6$	This work	$\text{SmBa}_2\text{Cu}_3\text{O}_6$
B_{20}	567(3)	633(3)	380(28)	282(5)	-730	-227
B_{40}	-2763(5)	-2741(6)	-2956(34)	-2481(12)	46	24
B_{44}	1470(5)	1466(5)	1664(25)	1307(10)	-350	-331
B_{60}	603(4)	618(5)	526(15)	321(12)	-115	-427
B_{64}	2283(4)	2233(5)	2021(10)	1931(6)	982	624

TABLE II. f - f transitions observed in $\text{Pr}_{1.05}\text{Ba}_{1.88}\text{Cu}_{2.39}\text{Al}_{0.34}\text{O}_{6+y}$ (sample 1) and $\text{Pr}_{0.93}\text{Ba}_{1.93}\text{Sr}_{0.13}\text{Mg}_{0.05}\text{Cu}_{2.74}\text{O}_{6+y}$ (sample 2), at $T = 10$ K, and the predicted energies obtained from a fit of the CF Hamiltonian. The CF levels for D_{4h} and C_{4v} are associated with the Pr^{3+} ion located in the regular site and the Ba site, respectively.

Multi-plet	Sample 1			Sample 2			Sample 2		
	Expt. (cm^{-1})	D_{4h} -symmetry site Theory (cm^{-1})	Sym. (Ref. 44) $i \Gamma_i$	Expt. (cm^{-1})	D_{4h} -symmetry site Theory (cm^{-1})	Sym. (Ref. 44) $i \Gamma_i$	C_{4v} -symmetry site Obs. (cm^{-1})	Calc. (cm^{-1})	
	0	0	3	0	2	5	0	3	
	7	6	5	10	11	3		83	
3H_4	383	394	2	372	378	2		122	
	410	401	1	400	389	1		208	
		609	5		614	4		292	
		614	4		618	5		411	
		827	1		830	1		525	
		2260	2249	1	2250	2239	1		2085
	2285	2288	2	2273	2272	2		2086	
	2346/59 ^a	2359	5	2342/56 ^a	2355	5		2112	
		2404	4		2410	4		2138	
3H_5	2580	2581	5	2557	2560	5		2225	
	2665	2660	3	2667	2666	3	2295	2288	
		2803	5	2806	2803	5		2369	
		2858	2		2863	2	2470	2476	
		4293	4294	5	4287	4290	5	4196	4193
		4332	4340	3	4336	4349	3	4231	4231
		4448	1		4442	1		4261	
3H_6	4504	4505	2	4499	4501	2	4323	4324	
	4615	4608	5	4611	4605	5	4385	4378	
		4696	4		4682	4		4464	
		4811	3	4808	4795	3		4509	
		4989	4993	5	5012	5003	5		4630
		5067	5066	1	5060	5074	1	4725	4735
	5105	5105	4	5114	5106	4	4739	4747	
3F_2	5471	5459	1	5471	5461	1	5255	5255	
	5516/24 ^a	5533	5	5517/28 ^a	5533	5	5279	5279	
		5601	3		5602	3		5374	
		5614	5614	4	5625	5625	4	5404	5400
		6527	6534	5	6530	6539	5	6460	6464
		6630	6621	3	6640	6631	3		6482
3F_3		6799	2		6793	2		6590	
		6909	5		6912	5		6607	
		7173	3		7173	3		6614	

^aThe doublet energies are approximated by their average value in the fitting procedure.

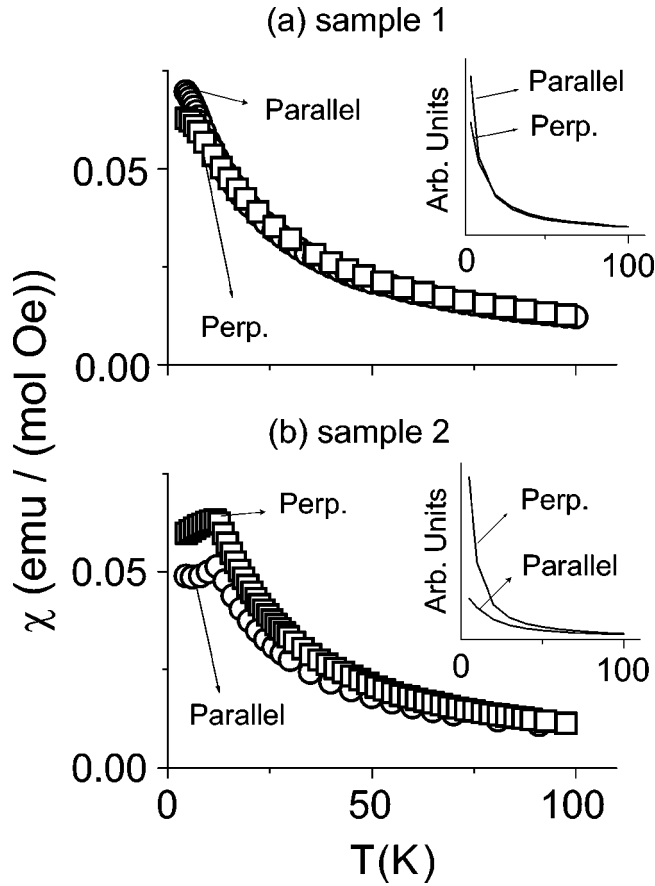


FIG. 6. Magnetic-susceptibility measurements of $\text{Pr}_{1.05}\text{Ba}_{1.88}\text{Cu}_{2.39}\text{Al}_{0.34}\text{O}_{6.35}$ (sample 1) and $\text{Pr}_{0.93}\text{Ba}_{1.93}\text{Sr}_{0.13}\text{Cu}_{2.74}\text{O}_{6.24}$ (sample 2) parallel (\parallel) and perpendicular (\perp) to the ab plane. Insets: calculations performed with the CF parameters reported in the 2nd and 3rd columns of the Table I.

Q -dependence study indicated that these peaks are mainly of phonon origin—though a very small magnetic contribution may underlie the phonon contribution.¹⁸

The comparison of the above-mentioned investigations of the CF interaction in $\text{PrBa}_2\text{Cu}_3\text{O}_{6+y}$ is hampered by several additional factors. First, the Pr substitution in the Ba site strongly depends on the sample preparation and is difficult to quantify. Second, the structural as well as the magnetic data including the CF excitations are more sensitive to oxygen content in comparison to the remaining members of the $\text{REBa}_2\text{Cu}_3\text{O}_{6+y}$ family.^{18,33,34} Third, Al^{3+} and Mg^{2+} ions contaminate the single crystals grown in Al_2O_3 (sample 1) and MgO (sample 2) crucibles by the flux technique.

Due to the over determination of the inverse secular problem we were able to determine a set of reliable phenomenological CF parameters of Pr^{3+} in $\text{Pr}_{1.05}\text{Ba}_{1.88}\text{Cu}_{2.39}\text{Al}_{0.34}\text{O}_{6+y}$ and $\text{Pr}_{0.93}\text{Ba}_{1.93}\text{Sr}_{0.13}\text{Mg}_{0.05}\text{Cu}_{2.74}\text{O}_{6+y}$. The comparison of our results with the $\text{NdBa}_2\text{Cu}_3\text{O}_6$ and $\text{SmBa}_2\text{Cu}_3\text{O}_6$ parameters (Table I) shows that the absolute value of B_{kq} tends to increase with the radial charge distribution $R_{4f}(r)$. As previously mentioned by Nekvasil,³⁵ these coefficients are generally higher than the CF parameters calculated for other RE oxides,³⁶ thus confirming the stronger contribution of CF interactions to the energy of the system. Also, the values of B_{20}

for D_{4h} -symmetry sites in samples 1 and 2 (Table I) compare reasonably well with the theoretical value of 425 cm^{-1} , calculated for the ideal $\text{PrBa}_2\text{Cu}_3\text{O}_6$ structure using the density-functional based method.^{11,12,37} The difference between our best-fit parameters and those reported by Hilscher *et al.*¹⁸ (e.g., $B_{20} = -317 \text{ cm}^{-1}$, $B_{40} = -2787 \text{ cm}^{-1}$, $B_{44} = 1098 \text{ cm}^{-1}$, $B_{60} = 864 \text{ cm}^{-1}$, and $B_{64} = 1446 \text{ cm}^{-1}$) is mainly ascribed to the misinterpretation of some of the above mentioned broad features in the INS spectra.

It is also interesting to note the energy splitting of the doubly degenerate Γ_5 levels at $T = 10$ and 78 K . Particularly evident for the $2242/56$ and $5517/28 \text{ cm}^{-1}$ features in Figs. 2 and 4, this phenomenon persists at $T = 78 \text{ K}$, far above the AFM ordering of the Pr sublattice. This band splitting is ascribed to an exchange interaction of the $4f$ electrons with the magnetically ordered Cu sublattice.² Moreover, the perfect isotropy of the low-temperature in-plane magnetization measurements, reported in the following, excludes the symmetry lowering as an alternative mechanism for the observed Γ_5 level splitting.

As for the effects of the Al doping, they manifest themselves by two remarkable features. Due to their localization in the $\text{Cu}(1)\text{O}(1)$ chains,³⁸ near the Ba site, the Al^{3+} ions are responsible for additional weak absorption peaks in $\text{Pr}_{1.05}\text{Ba}_{1.88}\text{Cu}_{2.39}\text{Al}_{0.34}\text{O}_{6+y}$, as indicated by the dashed vertical arrows in Figs. 3(a) and 3(b). We conjecture that these satellite absorption bands arise from Pr^{3+} ions occupying C_{4v} -symmetry Ba sites perturbed by neighboring Al^{3+} ions. On the other hand, the CF excitations associated with the D_{4h} -symmetry site of Pr^{3+} in $\text{Pr}_{1.05}\text{Ba}_{1.88}\text{Cu}_{2.39}\text{Al}_{0.34}\text{O}_{6+y}$ are shifted by $10\text{--}20 \text{ cm}^{-1}$ in $\text{Pr}_{0.93}\text{Ba}_{1.93}\text{Sr}_{0.13}\text{Mg}_{0.05}\text{Cu}_{2.74}\text{O}_{6+y}$ (Figs. 1–5). These shifts are associated with differences in the contribution of the long-range electrostatic interaction to B_{20} , which affects the high-order parameters only marginally.³⁹ In Table II the calculation of the CF levels reveals that the $\Gamma_5\text{--}\Gamma_1$ symmetry sequence of the quasitriplet ground state is reversed in $\text{Pr}_{1.05}\text{Ba}_{1.88}\text{Cu}_{2.39}\text{Al}_{0.34}\text{O}_{6+y}$ as compared to $\text{Pr}_{0.93}\text{Ba}_{1.93}\text{Sr}_{0.13}\text{Mg}_{0.05}\text{Cu}_{2.74}\text{O}_{6+y}$. As previously mentioned by Hilscher *et al.*,¹⁸ this reversal modifies the magnetic-susceptibility anisotropy at low temperature. In order to check this hypothesis and to further test the reliability of our theoretical approach, we have calculated the magnetic susceptibility using the CF parameters obtained for each sample. In addition to the AFM transition around $T_N = 12 \text{ K}$, the susceptibility measurements parallel (circles) and perpendicular (squares) to the ab plane show that $\chi_{\parallel} > \chi_{\perp}$ in $\text{Pr}_{1.05}\text{Ba}_{1.88}\text{Cu}_{2.39}\text{Al}_{0.34}\text{O}_{6.35}$ and $\chi_{\perp} > \chi_{\parallel}$ in $\text{Pr}_{0.93}\text{Ba}_{1.93}\text{Sr}_{0.13}\text{Cu}_{2.74}\text{O}_{6.24}$ [Figs. 6(a) and 6(b)]. Such reversal of the magnetic anisotropy is qualitatively reproduced by the calculations [inset of Figs. 6(a) and 6(b)] that do not include Pr-Pr anisotropic exchange and Pr-Cu interactions.^{2,20,40–42} In Fig. 6(b), it is noted that the Pr sublattice in sample 2 magnetically orders at $T_N(\text{Pr}) \sim 12 \text{ K}$. This value corresponds to the Néel temperature measured in polycrystalline low oxygenated materials.¹⁷ As expected,⁴³ the data reported in Fig. 6(a) show that the Al substitution of $\text{Cu}(1)$ in the chains suppresses $T_N(\text{Pr})$ in sample 1.

V. CONCLUSION

Using infrared transmission technique, we have detected 23 f - f transitions that involve the five lowest multiplets 3H_4 , 3H_5 , 3H_6 , 3F_2 , and 3F_3 multiplets of the Pr^{3+} ions in regular D_{4h} -symmetry sites in Al- and Sr-doped $\text{Pr}_{1+x}\text{Ba}_{2-x}\text{Cu}_3\text{O}_6$. A CF analysis of these transitions gives a good account of the experimental data including the magnetic-susceptibility anisotropy reversal. Regarding the $4f$ electrons radial charge distribution, our phenomenological CF parameters obtained for $\text{Pr}_{1.05}\text{Ba}_{1.88}\text{Cu}_{2.39}\text{Al}_{0.34}\text{O}_{6+y}$ and $\text{Pr}_{0.93}\text{Ba}_{1.93}\text{Sr}_{0.13}\text{Mg}_{0.05}\text{Cu}_{2.74}\text{O}_{6+y}$ follow the trends observed in $\text{NdBa}_2\text{Cu}_3\text{O}_6$ and $\text{SmBa}_2\text{Cu}_3\text{O}_6$. Additional absorption bands whose relative intensity and energy fluctuate as a function of the crystal stoichiometry are detected. We

assign these bands to the presence of Pr^{3+} ions in the irregular C_{4v} -symmetry sites resulting from Pr/Ba substitution.

ACKNOWLEDGMENTS

We thank J. Rousseau for his technical assistance. D.B. and S.J. acknowledge support from National Science and Engineering Research Council of Canada, Le Fonds de Formation de Chercheurs, and L'Aide à la Recherche du Gouvernement du Québec. Also are gratefully acknowledged the Grant Agency of the Czech Republic for its Grant No. 202/03/0552 (V.N., M.M., K.J., M.D.). The work performed in Prague was also supported by the institutional Project Nos. AV0Z1-010-914 and MSM113200002.

*Electronic address: dbarba@physique.usherb.ca

- ¹I. Felner, U. Yaron, I. Novik, E.R. Bauminger, Y. Wolfus, E.R. Yacoby, G. Hilscher, and Pillmayr, *Phys. Rev. B* **40**, 6739 (1990).
- ²A.T. Boothroyd, A. Longmore, N.H. Andersen, E. Brecht, and Th. Wolf, *Phys. Rev. Lett.* **78**, 130 (1997).
- ³V.P.S. Awana, C.A. Cardoso, O.F. de Lima, R. Singh, A.V. Narlikar, W.B. Yelon, and S.K. Malik, *Physica C* **316**, 113 (1999).
- ⁴H.A. Blackstead, J.D. Dow, I. Felner, and W.B. Yelon, *Phys. Rev. B* **63**, 094517 (2001).
- ⁵Z. Zou, J. Ye, K. Oka, and Y. Nishihara, *Phys. Rev. Lett.* **80**, 1074 (1998).
- ⁶I.I. Mazin, *Phys. Rev. B* **60**, 92 (1999).
- ⁷S.J.S. Lister, A.T. Boothroyd, N.H. Andersen, B.H. Larsen, A.A. Zhokhov, A.N. Christensen, and A.R. Wildes, *Phys. Rev. Lett.* **86**, 5994 (2001).
- ⁸V.E. Gasumyants, M.V. Elizarova, and R. Suryanarayanan, *Phys. Rev. B* **61**, 12 404 (2000).
- ⁹S.K. Malik, R. Prasad, N.N. Soni, K. Adhikary, and W.B. Yelon, *Physica B* **223-224**, 562 (1996).
- ¹⁰E. Brecht, P. Schweiss, Th. Wolf, A.T. Boothroyd, J.M. Reynolds, N.H. Andersen, H. Lütgemeier, and W.W. Schmahl, *Phys. Rev. B* **59**, 3870 (1999).
- ¹¹A.A. Martin, T. Ruf, M. Cardona, S. Jandl, D. Barba, V. Nekvasil, M. Diviš, and Th. Wolf, *Phys. Rev. B* **59**, 6528 (1999).
- ¹²D. Barba, S. Jandl, V. Nekvasil, M. Maryško, M. Diviš, A.A. Martin, C.T. Lin, M. Cardona, and Th. Wolf, *Phys. Rev. B* **63**, 054528 (2001).
- ¹³P. Allenspach, J. Mesot, U. Staub, M. Guillaume, A. Furrer, S.I. Yoo, M.J. Kramer, R.W. McCallum, H. Maletta, H. Blank, H. Mutka, R. Osborn, M. Arai, Z. Bowden, and A.D. Taylor, *Z. Phys. B: Condens. Matter* **95**, 301 (1994).
- ¹⁴M. Guillaume, W. Henggeler, A. Furrer, R.S. Eccleston, and V. Trounov, *Phys. Rev. Lett.* **74**, 3423 (1995).
- ¹⁵L. Soderholm, C.K. Loong, G.L. Goodman, and B.D. Dabrowski, *Phys. Rev. B* **43**, 7923 (1991).
- ¹⁶G.L. Goodman, C.K. Loong, and L. Soderholm, *J. Phys.: Condens. Matter* **3**, 49 (1991).
- ¹⁷H.D. Jostarndt, U. Walter, J. Kalenborn, A. Severing, and E. Holland-Moritz, *Phys. Rev. B* **46**, 14 872 (1992).
- ¹⁸G. Hilscher, E. Holland-Moritz, T. Holubar, H.D. Jostarndt, V. Nekvasil, G. Schaudy, U. Walter, and G. Fillion, *Phys. Rev. B* **49**, 535 (1994).
- ¹⁹V. Nekvasil, J. Stehno, J. Sebek, L. Havela, V. Sechovsky, and P. Svoboda, *J. Phys. (Paris), Colloq.* **49**, C8 (1988).
- ²⁰Th. Wolf, W. Goldacker, B. Obst, G. Roth, and R. Flükiger, *J. Cryst. Growth* **96**, 1010 (1989).
- ²¹C.T. Lin, A.M. Niraimathi, Y. Yan, K. Peters, H. Benders, E. Schönherr, and E. Gmelin, *Physica C* **272**, 285 (1996).
- ²²*Physical Properties of High Temperature Superconductors*, edited by Donald M. Ginsberg (World Scientific, Singapore, 1989), Vol. 1.
- ²³G. Bogachev, M. Abrashev, M. Iliev, N. Poulakis, E. Liarokapis, C. Mitros, A. Koufoudakis, and V. Psyharis, *Phys. Rev. B* **49**, 12 151 (1994).
- ²⁴M. Rübhausen, N. Dieckmann, A. Bock, and U. Merkt, *Phys. Rev. B* **54**, 14 967 (1996).
- ²⁵A.A. Mukhin, V.D. Travkin, S.P. Lebedev, A.S. Prokhorov, J. Hejtmanek, V. Nekvasil, and V. Zelezny, *J. Magn. Magn. Mater.* **531**, 177 (1998).
- ²⁶B.G. Wybourne, *Spectroscopic Properties of Rare Earths* (Interscience, New York, 1965).
- ²⁷V. Nekvasil, M. Diviš, G. Hilscher, and E. Holland-Moritz, *J. Alloys Compd.* **255**, 578 (1995).
- ²⁸U. Staub and L. Soderholm, in *Handbook on the Physics and Chemistry of Solids*, edited by J.K.A. Gschneider, Jr., L.R. Eyring, and M.B. Maple (Elsevier Science, New York, 2000), Vol. 30, pp. 491–545.
- ²⁹V. Nekvasil and M. Diviš, *Encyclopedia of Materials: Science and Technology* (Elsevier Science, New York, 2001), pp. 4613–4627.
- ³⁰G. Riou, S. Jandl, M. Poirier, V. Nekvasil, N. Diviš, P. Fournier, R.L. Greene, D.I. Zhigunov, and S.N. Barilo, *Eur. Phys. J. B* **23**, 179 (2001).
- ³¹M. Muroi and R. Street, *Physica C* **301**, 277 (1998).
- ³²M. Muroi and R. Street, *Physica C* **253**, 205 (1995).
- ³³A.T. Boothroyd, S.M. Doyle, and R. Osborn, *Physica C* **217**, 425 (1993).
- ³⁴M. Guillaume, P. Allenspach, J. Mesot, B. Roessli, U. Staub, P. Fischer, and A. Furrer, *Z. Phys. B: Condens. Matter* **90**, 13 (1990).
- ³⁵V. Nekvasil, *J. Magn. Magn. Mater.* **140**, 1265 (1995).
- ³⁶F. Auzel and O.L. Malta, *J. Phys. A* **44**, 201 (1983).

- ³⁷M. Diviš and V. Nekvasil, *Acta Phys. Pol.* **34**, 447 (2003).
- ³⁸E. Brecht, W.W. Schmahl, G. Miehe, M. Rodewald, H. Fuess, N.H. Andersen, J. Hansmann, and Th. Wolf, *Physica C* **265**, 53 (1996).
- ³⁹D.J. Newman and B. Ng, *Rep. Prog. Phys.* **52**, 699 (1989).
- ⁴⁰W.P. Wolf, *J. Phys. (Paris)* **32**, C1 (1971).
- ⁴¹S.V. Maleev, *JETP Lett.* **67**, 947 (1998).
- ⁴²A.A. Nugroho, V. Nekvasil, I. Veltruský, S. Jandl, P. Richard, A.A. Menovsky, F.R. de Boer, and J.J.M. Franse, *J. Magn. Magn. Mater.* **226-230**, 973 (2001).
- ⁴³H.D. Yang, M.W. Lin, C.K. Chiou, and W.H. Lee, *Phys. Rev. B* **46**, 1176 (1992).
- ⁴⁴G.F. Koster, J.O. Dimmock, R.C. Wheeler, and H. Statz, *Properties of the Thirty-Two Point Groups* (MIT Press, Cambridge, Massachusetts, 1963).